Optical absorption and electromagnetically induced transparency in semiconductor quantum well driven by intense terahertz field*

Wu Hong-Wei(吴宏伟) and Mi Xian-Wu(米贤武)†

College of Physical Science and Mechanical Engineering, Jishou University, Jishou 416000, *China*

(Received 19 March 2012; revised manuscript received 20 April 2012)

An approach for solving the excitonic absorption in a semiconductor quantum well driven by an intense terahertz field is presented. The formalism relies on the stationary single-photon Schrödinger equation in the full quantum mechanical framework. The optical absorption dynamics in both weak and strong couplings are discussed and compared. The excitonic absorption spectra show the Autler–Townes doublets for the resonance terahertz field, a replica peak for the non-resonance terahertz field, and the electromagnetically induced transparency phenomenon for modulating the decay rate of the second electron state in the weak coupling. In particular, the electromagnetically induced transparency phenomenon window range is discussed. In the strong coupling region，the multi-order energy level resonance splitting due to the strong optical field is found. There are three (non-resonance terahertz field) or four (resonance terahertz field) peaks in the optical absorption spectra. This work provides a simple and convenient approach to deal with the optical absorption in the exciton system.

Keywords: semiconductor quantum well, optical absorption spectrum, terahertz field, electromagnetically induced transparency

PACS: 71.35.Cc, 78.20.Jq, 71.70.Ej **DOI:** 10.1088/1674-1056/21/10/107102

1. Introduction

In recent years, the light-matter interaction has been a subject of intense and fruitful research, such as optical nonlinear absorption,[1−3] coherent population trapping (CPT),[4,5] electromagnetically induced transparency (EIT),[6−10] electromagnetically induced absorption,[11−14] lasing without inversion (LWI),[15] and giant Kerr nonlinear effect.[16,17] In particular, much attention has been devoted to studying the interaction of the light with the semiconductor quantum well (QW).[18−27] The achievement may lead to the implementation of optical switches and optical modulators based on the tunable excitonic absorption. Some of those investigations are aimed at exploring the optical absorption properties at the near band edge in the semiconductor QW system. It is well known that the interband absorption and the intersubband absorption or emission[28−31] in an undoped QW can be modified by an intense far-infrared laser beam polarizing along the growth direction. The quantum-confined Stark effect (QCSE)[32] occurs for the intense far-infrared laser driven dipole transitions between two electron subbands or two hole subbands. The terahertz (THz) field, which is applied to tune the interband absorption[33] of the semiconductor, is particularly interesting. The intersubband transition frequency in the conduction band or the valence band falls in the frequency range of the THz field.

There have been a large number of efforts made to theoretically study the optical absorption in the semiconductor QW system driven by an intense THz field. To study the dynamical Franz–Keldysh effect of the optical absorption[34,35] in the QW system, the THz wave is applied in the QW layer plane, the intersubband (1s–2p) transition is realized in the semiconductor QW. When an intense far-infrared field only drove two conduction subbands, the optical absorption in a symmetric QW system was investigated by Liu and Ning.[36] Maslov and Citrin[37] calculated the optical absorption of the light interacting with an infinitely deep single QW system when only two valence subbands were tuned by the THz field. The Autler–Townes (AT) splitting in the optical absorp-

*Project supported by the National Natural Science Foundation of China (Grant No. 10647132) and the Science Foundation from the Education Department of Hunan Province, China (Grant No. 10A100).

†Corresponding author. E-mail: xwmi@yahoo.com.cn

© 2012 Chinese Physical Society and IOP Publishing Ltd

tion spectrum has been observed in the above study for the resonance far-infrared or THz field. In particular, Maslov and Citrin found that replicas and a sideband[38] emerged for a low frequency THz field coupling with the subbands. The features of the first and the second order Stark effects were shown in that study. The authors also studied the case of a strong direct-current (dc) bias mixing with the THz field, and the multi-replica emerged on both sides of the main absorption peaks. Recently, Zhang and Allsopp[39] improved the model of interband absorption for the asymmetric semiconductor double QWs. The work was based on the study of the Maslov group. The interband absorption of the asymmetric semiconductor double QWs driven by an intense THz field has been explored. Several factors were considered in the discussion of the optical absorption, such as the near-infrared (NIR) beam energy, the frequency and the intensity of the THz field. The absorption spectra showed peak variations due to the Coulombic coupling effect and the multi-order Stark effect. For asymmetric semiconductor double QWs, they comprehensively studied the replica and sideband phenomenon between near-resonance and non-resonance THz cases. However, they dealt with the semiconductor QW system with the semi-classical method, whereas the probe beam and the THz field were treated in the classical form. Many questions of the interband absorption remain unresolved in the region where the NIR probe beam strongly interacts with the QW system in the presence of an intense THz field.

Generally, various results of interband absorption for the NIR beam interacting with the QW system are obtained with the aid of semiconductor Bloch equation.[39] In Ref. [39], the excitonic absorption in the asymmetric double QWs driven by an intense terahertz field was obtained by solving the Heisenberg moving equation of interband polarization. Though the results of excitonic absorption in the semiconductor QW have been reported many times, a large proportion of the results were obtained in the semi-classical framework. Due to the development of the quantum mechanics and a deeper understanding of the theory of quantum dynamics, a full quantum Hamiltonian of the optical field and the interaction term between the optical field and the semiconductor QW system was obtained by Kira and Koch.[40] Understanding of the physics underlying the light-QW interaction for the excitonic absorption in the QW system is important in the calculation and analysis of their absorption features. The exciton (electron and hole pair) is formed because the photons stimulate the electron transition from the valence band to the conduction band. For this reason, we can obtain the optical absorption coefficient from the probability amplitude of the excitonic state. This basic idea has been perfectly applied to calculate the photon transmission and reflection coefficient for photon scattering by a three-level emitter in a one-dimensional waveguide.[41,42]

In this work, the stationary single-photon Schrödinger equation is employed to study the excitonic absorption in the semiconductor QW in the full quantum regime. The merit of this approach is that we not only easily obtain the evolutions of the optical absorption spectra by governing the detuning, but also more conveniently and accurately study the multi-feature of the optical properties. In order to obtain the rich features of the interband optical absorption, we set up a three-level system (TLS) in the semiconductor QW. The absorption peak shows a symmetric evolution feature when the detuning changes from a negative value to a positive one. The Autler–Townes double peaks emerge when the detuning is zero (i.e., the THz field frequency equals the transition frequency between the first electron subband and the second electron subband) due to the optical Stark effect (OSE). When we increase the coupling strength of the THz field, the space between the two main peaks of the AT splitting becomes very large. Simultaneously, the EIT phenomenon emerges when the decay rate is decreased to zero in the resonance THz field. The transparency window (TW) is tuned by changing the coupling constant of the THz field. When increasing the coupling constant of the probe beam, the multi-resonance phenomenon occurs, and the absorption spectrum of the QW system shows that two small peaks emerge between the two main peaks in the presence of resonance-THz field for the large NIR coupling constant. The multi-absorption peaks emerge with the change of the THz frequency in the strong coupling region. This method may become an effective way for solving the excitonic absorption in the semiconductor QW, and the results may help to realize an optical detector and converter.

2. Model and solution

The method of stationary single-photon Schrödinger equation has been successfully applied

to the calculation of transmission and reflection coefficients in a one-dimensional waveguide. Now, we adopt it to study the optical absorption properties of the semiconductor QW. The electron and the hole states of the semiconductor QW are calculated by using the $\boldsymbol{k}\cdot\boldsymbol{p}$ perturbation theory. We can write the single particle Hamiltonian as

$$H(r) = -\frac{(\partial_x^2+\partial_y^2)}{2m_{\parallel}^*(x,y)} - \frac{\partial_z^2}{2m_{\perp}^*(z)} + V(z),$$

where $m_{\parallel}^*(x,y)$ is the effective mass for the motion in the QW layer plane, $m_{\perp}^*(z)$ is the effective mass for the motion along the z direction of the QW. We set $\hbar = 1$ in this paper. The $V(z)$ is the potential energy, which is determined by the band offsets of the conduction (or valence) band in the QW region. We can obtain the electron envelope function $|\varphi_{nk}^{\rm e}(\boldsymbol{r})\rangle$ and eigenenergy $\varepsilon_n^{\rm e}$ (the hole envelope function $\left|\psi_{lk}^{\rm h}(\boldsymbol{r})\right\rangle$ and eigenenergy $\varepsilon_l^{\rm h}$) by solving a set of secular equations, which comes from the eigenequation by imposing the periodic boundary condition, where n and l are the indexes of the conduction and the valence subbands, respectively.

We consider a typical TLS system, an NIR probe beam couples with the first electron subband and the first hole subband ($X_{\rm e1h1}$), and a strong THz beam couples with the first and the second electron subbands. We prohibit the transition from the first hole subband to the second electron subband by the NIR excitation for exactly exploring the cases of excitonic absorption in this system, because the exciton $X_{\rm e1h1}$ has much larger optical dipole matrix elements than the exciton $X_{\rm e2h1}$ (the second electron subband and the first hole subband) ($|\mu_{11k}| \approx 3\,|\mu_{21k}|$).[39] The Hamiltonian of the TLS system in second quantization in the presence of the optical field (NIR probe beam) and the THz laser can be written as $H = H_{\rm opt} + H_{\rm 3LS} + H_{\rm c}$, where $H_{\rm opt}$ and $H_{\rm 3LS}$ represent the free photons and the three-level system, respectively, $H_{\rm c}$ denotes the interaction term between the probe beam and the TLS. The free photons are described for considering the contribution of positive and negative photon momenta[41] as

$$H_{\rm opt} = -{\rm i}c_g \sum_{j=1,2}\int {\rm d}x a_j^{\dagger}(x)\partial_x a_j(x), \qquad (1)$$

where $c_{\rm g}$ is the group velocity of the photons, and we set $c_{\rm g} = 1$ for simplicity, $j = 1,2$ represent respectively the positive and the negative free photon momenta, $a_j^{\dagger}$ (a_j) denotes the creation (annihilation) operator of photons with the negative or positive momenta in the photon incidence direction. We consider the TLS consisted of two upper states $|\varphi_{1k}^{\rm e}(\boldsymbol{r})\rangle = \lambda G_1(z)\,{\rm e}^{{\rm i}\boldsymbol{k}\cdot\boldsymbol{\beta}}$, $|\varphi_{2k}^{\rm e}(\boldsymbol{r})\rangle = \lambda G_2(z)\,{\rm e}^{{\rm i}\boldsymbol{k}\cdot\boldsymbol{\beta}}$ and one lower state $\left|\psi_{1k}^{\rm h}(\boldsymbol{r})\right\rangle = \lambda R_1(z)\,{\rm e}^{{\rm i}\boldsymbol{k}\cdot\boldsymbol{\beta}}$. The $|\varphi_{2k}^{\rm e}(\boldsymbol{r})\rangle$ of the TLS is coupled to state $|\varphi_{1k}^{\rm e}(\boldsymbol{r})\rangle$ by a THz beam with Rabi frequency $\Omega_{\rm THz}$ and detuning Δ. We set the energy of the lower state $\left|\psi_{1k}^{\rm h}(\boldsymbol{r})\right\rangle$ to zero as the reference for simplicity. The λ is the area parameter of the QW plane, $\boldsymbol{\beta}$ is the two-dimensional (2D) in-plane position vector, $G_{nk}^{\rm e}(z)$ and $R_{lk}^{\rm h}(z)$ denote the confinement envelope functions of electron and hole in the z direction corresponding to energies $\varepsilon_n^{\rm e}$ and $\varepsilon_l^{\rm h}$, respectively. Thus, the TLS Hamiltonian in the rotating wave approximation is written as

$$H_{\rm 3LS} = \begin{pmatrix} (E_{1k}^{\rm e} - {\rm i}\gamma_1/2)C_{1k}^{\dagger}C_{1k} \\ +(E_{1k}^{\rm e} + \Delta + \omega_{\rm THz} - {\rm i}\gamma_2/2)C_{2k}^{\dagger}C_{2k} \\ +\Omega_{\rm THz}(C_{1k}^{\dagger}C_{2k} + C_{2k}^{\dagger}C_{1k}) \end{pmatrix}, \quad (2)$$

where

$$E_{1k}^{\rm e} = \varepsilon_1^{\rm e} + \frac{k^2}{2m_{\rm e\parallel}^*} + E_{\rm g} + \varepsilon_1^{\rm h} + \frac{k^2}{2m_{\rm h\parallel}^*}$$

is the energy of the upper state $|\varphi_{1k}^{\rm e}(\boldsymbol{r})\rangle$, $C_{2k}^{\dagger}$ and C_{2k} ($C_{1k}^{\dagger}$ and C_{1k}) are the creation and the annihilation operators for the electron in state $|\varphi_{2k}^{\rm e}(\boldsymbol{r})\rangle$ ($|\varphi_{1k}^{\rm e}(\boldsymbol{r})\rangle$), respectively, ${\rm i}\gamma_2/2$ and ${\rm i}\gamma_1/2$ are the decay parts from $|\varphi_{2k}^{\rm e}({\rm r})\rangle$ and $|\varphi_{1k}^{\rm e}(\boldsymbol{r})\rangle$ due to the spontaneous emission. The NIR beam interacts with the TLS in the QW at $x = 0$. The interaction Hamiltonian term can be written as

$$H_{\rm c} = \sum_{j=1,2}[\Omega_{\rm NIR}a_j^{\dagger}(0)S_- + \Omega_{\rm NIR}^*S_+a_j(0)], \qquad (3)$$

where S_+ (S_-) is the creation (annihilation) operator of the electron–hole pair, $\Omega_{\rm NIR}$ denotes the Rabi frequency for the NIR beam interacting with the exciton $X_{\rm e1h1}$.

The Hamiltonian of the full system is simplified by using the (anti)-symmetric transformation. The relation equations $a_{\rm even}(x) = [a_1(x) + a_2(-x)]/\sqrt{2}$ and $a_{\rm odd}(x) = [a_1(x) - a_2(-x)]/\sqrt{2}$ are introduced.[41] In the transformation basis, the full Hamiltonian is split into the part which contains the interaction term between the even modes with the TLS and the part of noninteracting odd mode optical field. We structure the single-photon eigenstates of the full system as

$$|\Psi\rangle = \begin{pmatrix} \dfrac{B_{\rm even}}{\sqrt{2\pi}} \displaystyle\int \mathrm{d}x \begin{bmatrix} A_{1k}(x) a^{\dagger}_{\rm even}(x) \left|0, \psi^{\rm h}_{1k}(\boldsymbol{r})\right\rangle \\ +A_{2k} \left|0, \varphi^{\rm e}_{1k}(\boldsymbol{r})\right\rangle + A_{3k} \left|0, \varphi^{\rm e}_{2k}(\boldsymbol{r})\right\rangle \end{bmatrix} \\ +\dfrac{B_{\rm odd}}{\sqrt{2\pi}} \displaystyle\int \mathrm{d}x \left[A_{4k}(x) a^{\dagger}_{\rm odd}(x) \left|0, \psi^{\rm h}_{1k}(\boldsymbol{r})\right\rangle\right] \end{pmatrix}, \tag{4}$$

where

$$B_{\rm even} = 1/\sqrt{2}(1/\sqrt{2}), \quad B_{\rm odd} = 1/\sqrt{2}(-1/\sqrt{2})$$

are for the incoming photons from the left (right) of the TLS, A_{ik} is the excitation amplitude of the i-th state. The $|0, -\rangle$ denotes zero photon in the state of the TLS. We obtain different coefficients of the eigenstates by solving the stationary single-model optical Schrödinger equation with $A_{1k}(0) = [A_{1k}(0-) + A_{1k}(0+)]/2$, while the photon is a single plane wave before interacting with the TLS. Here, the absorption coefficient is obtained by solving the stationary single-photon Schrödinger equation, and we write the absorption coefficient as

$$\sigma(\omega_{\rm NIR}) = \frac{1 - \Upsilon_k^2}{2}, \tag{5}$$

where

$$\Upsilon_k = \frac{(2\Xi - \mathrm{i}\Omega^2_{\rm NIR})^2}{4\Xi^2 + \Omega^4_{\rm NIR}},$$

$$\Xi = \frac{(\omega_{\rm NIR} - E^{\rm e}_{1k} + \mathrm{i}\gamma_1/2)\left[4\left(\omega_{\rm NIR} - E^{\rm e}_{1k} - \Delta - \omega_{\rm THz} + \mathrm{i}\gamma_2/2\right)\right] - \Omega^2_{\rm THz}}{4\left(\omega_{\rm NIR} - E^{\rm e}_{1k} - \Delta - \omega_{\rm THz} + \mathrm{i}\gamma_2/2\right)}.$$

The parameters[43] for the GaAs QW at low temperatures are $m^*_{\rm e\|} = m^*_{\rm e\perp} = 0.067m_0$, $m^*_{\rm h\|} = 0.109m_0$, $m^*_{\rm h\perp} = 0.34m_0$ (m_0 is the free-electron mass), and $E_{\rm g} = 1.424$ eV. The well width of the GaAs QW is 150 Å (1 Å=0.1 nm). The temporal pulse of the NIR is 20 fs, and the lattice temperature is set to $T = 77$ K.

3. Discussion

Exploiting the above results, we can analyze the dynamical behavior of the optical absorption of the TLS and compare the results for different THz coupling constant, NIR coupling strength, decay rates of various electron subbands, and detuning. In fact, several authors have obtained optical absorption features using the semiconductor Bloch equation. Our results are given by using the stationary single-photon Schrödinger equation in the quantum framework. We can know that the absorption coefficient is proportional to the square of coefficient A_{2k} of the first electron state. We discuss the optical absorption dynamic and sort the results according to the different coupling strengths of the NIR probe beam (weak and strong interactions).

3.1. Weak interaction

Figure 1 shows the optical absorption spectra of the TLS for different detunings. A small replica peak is found at the left side of the main peak for $\Delta = -0.3$ eV. The replica peak moves to the main peak for the near-resonance THz field by adjusting the detuning. When the detuning is tuned to zero, the first electron state is split into two dressing states by the resonance THz field, the replica peak vanishes, and the main peak is split into two equal-magnitude peaks, which is the AT double-peak phenomenon. In fact, the result is that the carriers are redistributed by the THz field. The AT double peaks become two asymmetric peaks and one of them becomes smaller with the increasing detuning. When we continue to increase the detuning, the replica peak appears in the optical

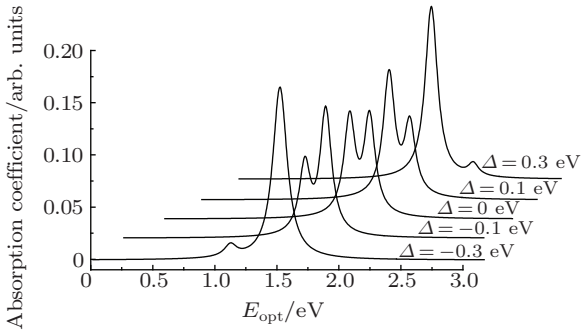


Fig. 1. Absorption spectra measured with the NIR beam in the presence of the THz field for the NIR beam coupling constant $\Omega_{\rm NIR} = 0.1$ meV, the decay rates of states $\gamma_2 = 0.1$ meV and $\gamma_1 = 0.1$ meV, the THz field frequency $f_{\rm THz} = 3.8$ THz, and the THz field coupling strength $\Omega_{\rm THz} = 3$ meV.

absorption spectrum again, but the replica peak is located at the right side of the main peak, because the detuning is set at a positive value. When the detuning increases from $\Delta = 0.3$ eV to a greater value, the replica peak moves to the far right hand side of the main peak, and the magnitude of the replica peak becomes smaller. The theoretical results are consistent with the experimental results.

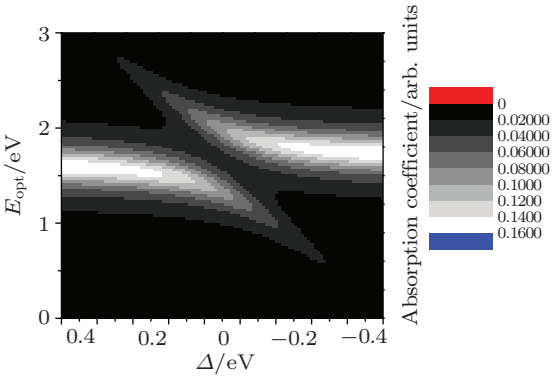


Fig. 2. Plane-three-dimensional plot of absorption spectrum on the optical field frequency and detuning, the parameters are $\Omega_{\rm NIR} = 0.1$ meV, $\gamma_2 = 0.1$ meV, $\gamma_1 = 0.1$ meV, $f_{\rm THz} = 3.8$ THz, and $\Omega_{\rm THz} = 3$ meV.

In Fig. 2, it is not difficult to find that the absorption spectrum evolution is symmetric for the detuning from the negative value to the positive one. The pronounced absorption single peaks emerge at the vicinities of the left ($E_{\rm opt} = 1.5555$ eV, $\Delta = 0.45$ eV) and the right ($E_{\rm opt} = 1.5555$ eV, $\Delta = -0.45$ eV) sides for the large detuning. When the absolute value of the detuning is decreased, a replica peak is found in Fig. 2. When the detuning is decreased to $\Delta = 0.0$ eV, the equal-magnitude double peaks emerge at $E_{\rm opt} = 1.300$ eV and $E_{\rm opt} = 1.811$ eV. The feature indicates that the intensity of the main peak becomes weaker and the small replica peak becomes stronger when the THz field frequency is close to the frequency difference between the first and the second electron states.

Having investigated the interband absorptions for different detunings, we now explore the absorption coefficients with different THz field coupling constants. In Fig. 3, it is shown that these features only depend on the coupling strength of the THz field. Varying the coupling strength of the THz field causes a significant change in the shape of the optical absorption feature, which evolves from a single peak to the equal-magnitude double peaks. Figure 3(a) shows the single absorption peak in the optical absorption spectrum with the absence of the THz field at $E_{\rm opt} = 1.5555$ eV, this is because the energy of the first electron state is 1.5555 eV. We now proceed to increase the THz coupling constant to study the evolution of the absorption peaks.

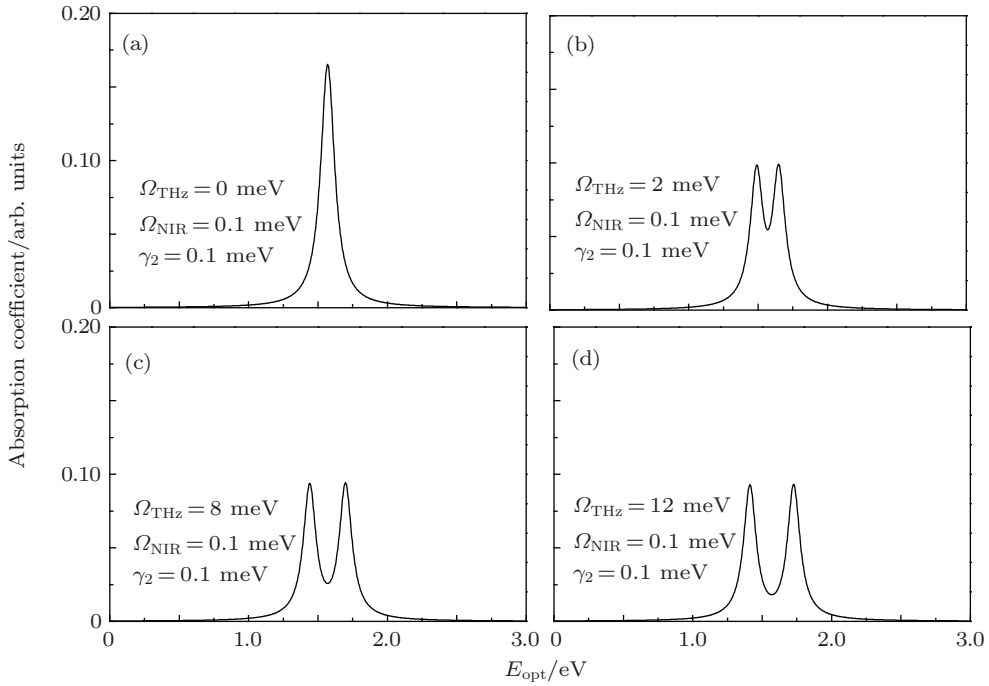


Fig. 3. The optical absorption spectra for different THz field couplings: (a) $\Omega_{\rm THz} = 0$ meV, (b) $\Omega_{\rm THz} = 2$ meV, (c) $\Omega_{\rm THz} = 8$ meV, and (d) $\Omega_{\rm THz} = 12$ meV, where $\gamma_2 = 0.1$ meV, $\Delta = 0$ eV, and the other parameters are the same as before.

In Fig. 3(b), the main peak is split into two smaller peaks when the coupling constant is $\Omega_{\rm THz} = 2$ meV. This is the Aulter–Townes splitting, the manifestation of the resonance THz field. In Figs. 3(c) and 3(d), the exciton peaks may be resolved clearly. We observe that as the THz field coupling strength increases, the dip between the two main peaks becomes deeper and broader. Comparing Fig. 4 to Fig. 3, we find that the optical absorption spectrum shows a dramatic phenomenon (EIT) when the decay rate of the second electron subband is decreased. The electromagnetically induced transparency phenomenon becomes visible and obvious when the decay rate is zero and the coupling constant of the resonance THz field becomes much larger. The EIT window becomes broader with the increasing coupling strength.

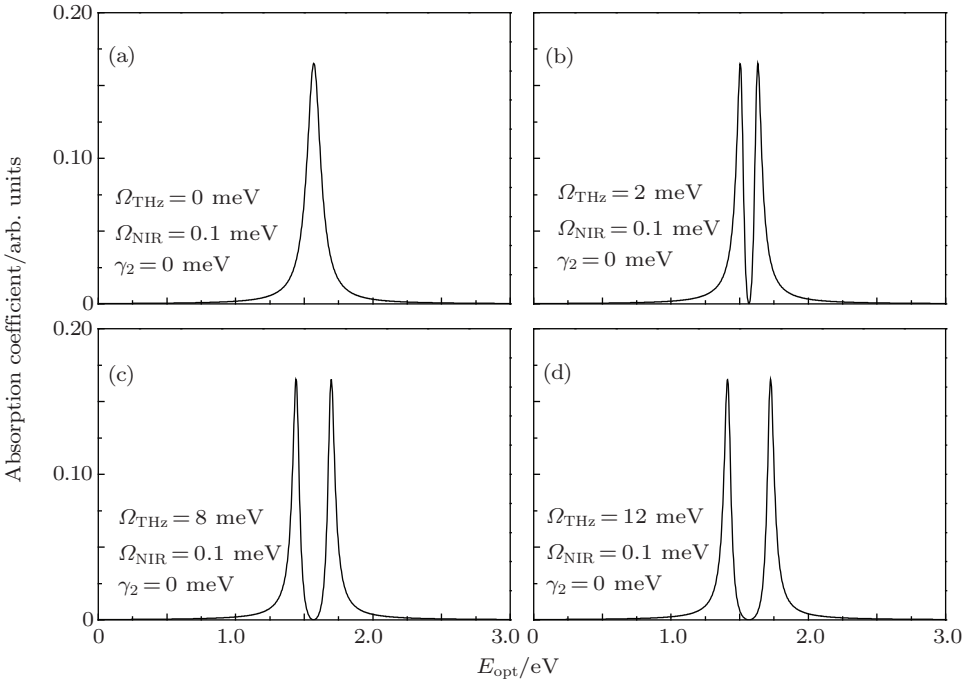


Fig. 4. The optical absorption spectra (EIT absorption spectrum) for different THz field couplings: (a) $\Omega_{\rm THz} = 0$ meV, (b) $\Omega_{\rm THz} = 2$ meV, (c) $\Omega_{\rm THz} = 8$ meV, (d) $\Omega_{\rm THz} = 12$ meV, where $\gamma_2 = 0.0$ meV, $\Delta = 0$ eV, and the other parameters are the same as before.

3.2. Strong interaction

Now we study the absorption features in the presence of intense THz driving field and the strong NIR in the semiconductor QW.

In Fig. 5, we demonstrate the optical absorption features for different NIR coupling constants ($\Omega_{\rm NIR} = 0.02$ eV, $\Omega_{\rm NIR} = 0.04$ eV, $\Omega_{\rm NIR} = 0.06$ eV, $\Omega_{\rm NIR} = 0.09$ eV) in the presence of the resonance THz field ($\Delta = 0.0$ eV). The AT double peaks emerge in the optical absorption spectrum when the optical coupling constant is $\Omega_{\rm NIR} = 0.02$ eV. When the coupling constant of the NIR beam is increased, the left one of the double peaks is red-shifted, but the right one is blue-shifted, and the peak magnitude is increased. However, the interesting features are in the interpeak dip. One remarkable feature is that two small peaks emerge in the dip when $\Omega_{\rm NIR} = 0.04$ eV. For increasing $\Omega_{\rm NIR}$, the small peaks become bigger, and the separation between the two small peaks becomes narrower. When $\Omega_{\rm NIR} = 0.02$ eV, two main peaks emerge at $E_{\rm opt} = 1.49$ eV and $E_{\rm opt} = 1.61$ eV. However, two dips emerge at $E_{\rm opt} = 1.49$ eV and $E_{\rm opt} = 1.61$ eV when $\Omega_{\rm NIR} = 0.09$ eV. Similarly, the intensity of the main absorption peak becomes stronger with the increasing optical coupling constant. For the dramatic changes, the physics underlying is that the two splitting energy levels from electron state $|\varphi^{\rm e}_{1k}({\rm r})\rangle$ due to the resonance THz field are split into four sublevels (the second order dressing state) for the strong resonance NIR probe beam. The two internal sublevels are nearly together and the two external sublevels become further separated for the increasing coupling constant. Thus, the locations of the emerging absorption peaks in the weak coupling region evolve into two deep dips

in the strong coupling region. When $\Omega_{\rm NIR} = 0.11$ eV, the two internal sublevels move to merge to form a big absorption peak in the optical absorption spectrum (not shown in Fig. 5).

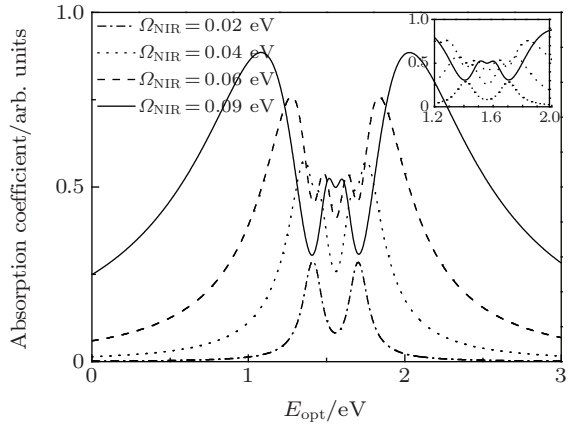


Fig. 5. The interband absorptions for different coupling constants of the NIR probe beam: $\Omega_{\rm NIR} = 0.02$ eV, $\Omega_{\rm NIR} = 0.04$ eV, $\Omega_{\rm NIR} = 0.06$ eV, $\Omega_{\rm NIR} = 0.09$ eV in the near-resonance THz ($\Delta = 0.0$ eV) and the THz coupling constant ($\Omega_{\rm THz} = 5$ meV), the other parameters are the same as before. The insert figure is the optical absorption spectrum for the optical frequency from 1.2 eV to 2.0 eV.

As the THz field can tune the electron transition between two subbands in the TLS, we now consider the optical absorptions with different THz field frequencies when $\Omega_{\rm NIR} = 0.05$ eV and $\Omega_{\rm THz} = 5$ meV, as shown in Figs. 6 and 7.

Two pronounced peaks and a small peak are found in the optical absorption spectrum in Fig. 6(a). The two main peaks come from the first electron state for the strong NIR beam probing ($\Omega_{\rm NIR} = 0.05$ eV), and the ground state has no splitting for the resonance NIR beam. The small peak is the result of the carriers being stimulated from the second electron state by the high frequency THz field. When $\Delta = -0.2$ eV and the other parameters are the same as before, the small peak merges to the left one of the two main peaks, and the magnitude of the left main peak becomes small; the right one is unchanged. This phenomenon is because the THz frequency is near the transition frequency between the second electron state and the lower one of the two dressing states of the first electron state. When the THz frequency is decreased to the transition frequency between the two electron states of the bare system (i.e. $\Delta = 0.0$ eV), two small replica peaks are observed in the dip between the two main peaks in Fig. 6(d). This is because the THz frequency , though it is greater than the transition frequency between the upper dressing state and the second electron state, is less than the lower one. The absorption peak for the nonresonance THz field becomes small compared to the case of resonance.

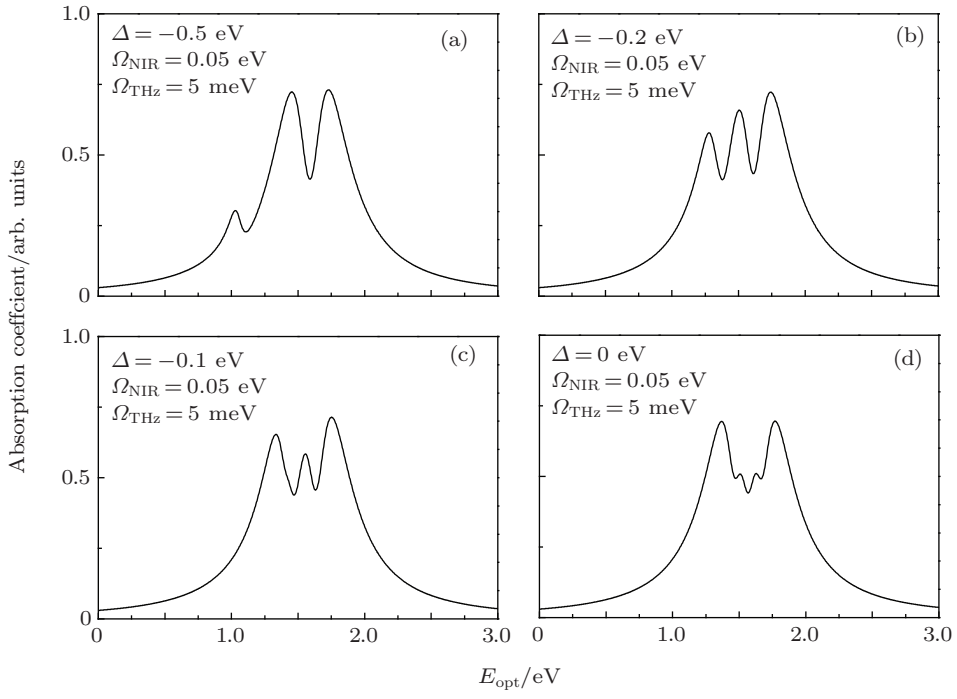


Fig. 6. The interband absorption spectra with (a) $\Delta = 0.5$ eV, (b) $\Delta = 0.2$ eV, (c) $\Delta = 0.1$ eV, and (d) $\Delta = 0$ eV are shown for $\Omega_{\rm NIR} = 0.05$ eV and $\Omega_{\rm THz} = 5$ meV in the region of THz frequency near the transition frequency between the second electron state and the low-energy dressing state from the first electron state.

Figure 7 shows the evolution process of the right peak with the decreasing THz frequency in the low frequency region. The left main peak recovers, and the small replica peak emerges at the left side of the right main peak, because the distribution of carriers is changed when the detuning is changed from $\Delta = 0.0$ eV to $\Delta = 0.1$ eV. Two equal altitude small peaks emerge when the THz frequency equals the transition frequency between the second electron state and the upper dressing state (not shown in Fig. 7). The asymmetric double peaks are obtained again and the replica locates at the right side of the main peaks in Fig. 7(c). In Fig. 7(d), the two main peaks recover to the shapes of a non perturbative case, and the replica moves far to the right.

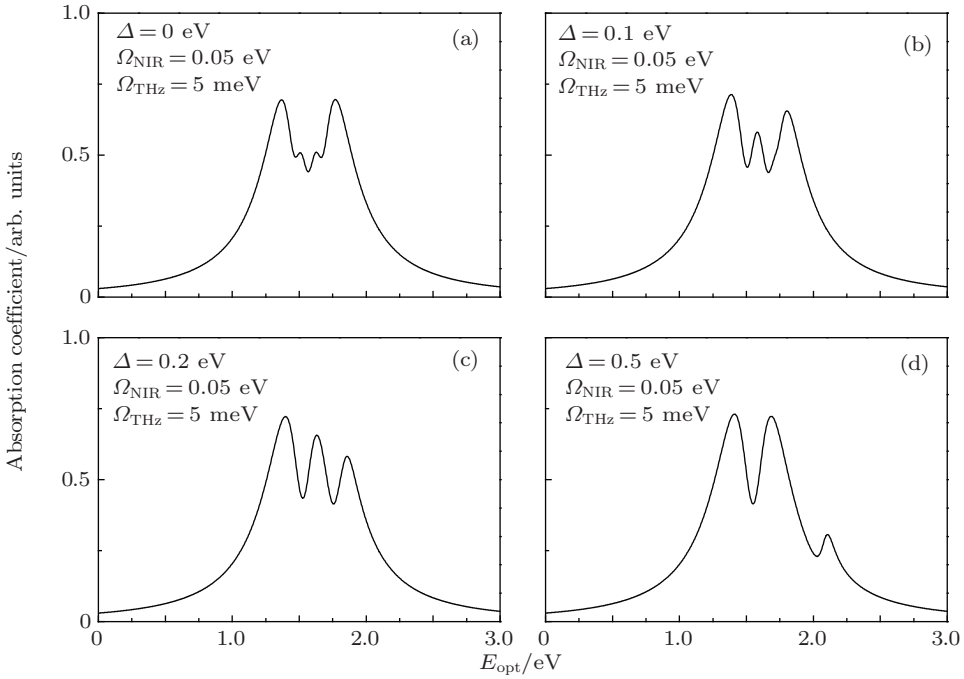


Fig. 7. The interband absorption spectra with (a) $\Delta = 0$ eV, (b) $\Delta = 0.1$ eV, (c) $\Delta = 0.2$ eV, and (d) $\Delta = 0.5$ eV are shown for $\Omega_{\rm NIR} = 0.05$ eV and $\Omega_{\rm THz} = 5$ meV in the region of THz frequency near to the transition frequency between the second electron state and the high-energy dressing state from the first electron state.

4. Conclusion

In summary, the optical absorption dynamics are obtained by solving the stationary single-photon Schrödinger equation, which is much simpler than the other approaches.[38,44] The formalism shows the quantum process of the interaction between the optical field and the QW system. With realistic parameters, in weak coupling, the optical absorption spectrum shows the AT doublets for the resonance THz field, a replica peak for the non-resonance THz field, and the EIT phenomenon for modulating the decay rate of the second electron state. Particularly, the EIT window range only depends on the coupling constant. In strong coupling, when the coupling constant of the NIR probe beam is increased for the same resonance THz field, the absorption spectrum shows that the former main peaks blue/red shift, respectively, small replica peaks emerge and merge together. We note that there are replica (non-resonance THz field) and replica-main peak transitions (resonance THz field) in the optical absorption spectra. The results may be useful for the investigation of optical devices. Our approach may become a powerful tool for solving the optical absorption properties of semiconductor well systems.

References

[1] Monozon B S and Schmelcher P 2010 *Phys. Rev.* B **82** 205313

[2] Batista A A, Tamborenea P I, Birnir B, Sherwin M S and Citrin D S 2002 *Phys. Rev.* B **66** 195325

[3] Liu H C and Springtharpe A J 2000 *Phys. Rev.* B **61** 15629

[4] Alzetta G, Gozzini A, Moi L and Orriols G 1976 *Nuovo Cimento* B **36** 5

[5] You S P, Liu Z D, Pang W, Cheng J and Zheng J 2010 *Chin. Phys.* B **19** 044201

[6] Sun Q, Rostovtsev Y V, Dowling J P, Scully M O and Zubairy M S 2005 *Phys. Rev.* A **72** 031802(R)

[7] Schmidt H, Campman K L, Gossard A C and Imamoglu A 1997 *Appl. Phys. Lett.* **70** 3455

[8] Phillips M and Wang H L 2002 *Phys. Rev. Lett.* **89** 186401

[9] Silvestri L, Bassani F, Czajkowski G and Davoudi B 2002 *Eur. Phys. J.* B **27** 89

[10] Li T, Wang H L, Kwong N and Binder R 2003 *Opt. Express* **11** 3298

[11] Wang L and Hu X M 2004 *Acta Phys. Sin.* **53** 2551 (in Chinese)

[12] Li X L, Yang B Z, Yang L J and Zhang L S 2010 *Acta Phys. Sin.* **59** 7008 (in Chinese)

[13] Yan X A, Song J P and Zhang Y P 2008 *Acta Phys. Sin.* **57** 3538 (in Chinese)

[14] Wang L and Lu C 2011 *Acta Phys. Sin.* **60** 044203 (in Chinese)

[15] Liu Z B, Liang Y, Jia K N and Fan X J 2012 *Chin. Phys.* B **21** 024206

[16] Schmidt H and Imamoglu A 1996 *Opt. Lett.* **21** 1936

[17] Kang H and Zhu Y 2003 *Phys. Rev. Lett.* **91** 093601

[18] Imamoglu A and Ram R J 1994 *Opt. Lett.* **19** 1744

[19] Faist J, Capasso F, Sirtori C, West K W and Pfeiffer L N 1997 *Nature* **390** 589

[20] Potz W 1997 *Phys. Rev. Lett.* **79** 3262

[21] Ku P C, Sedgwick F, Chang-Hasnain C J, Palinginis P, Li T, Wang H L, Chang S W and Chuang S L 2004 *Opt. Lett.* **29** 2291

[22] Frogley M D, Dynes J F, Beck M, Faist J and Phillips C C 2006 *Nat. Mater.* **5** 175

[23] Wu J H, Gao J Y, Xu J H, Silvestri L, Artoni M, LaRocca G C and Bassani F 2006 *Phys. Rev.* A **73** 053818

[24] Li J H 2007 *Phys. Rev.* B **75** 155329

[25] Yang W X, Hou J M and Lee R K 2008 *Phys. Rev.* A **77** 033838

[26] Zhu C J and Huang G X 2009 *Phys. Rev.* B **80** 235408

[27] Serapiglia G B, Paspalakis E, Sirtori C, Vodopyanov K L and Phillips C C 2000 *Phys. Rev. Lett.* **84** 1019

[28] Williams B S, Xu B, Hu Q and Melloch M R 1999 *Appl. Phys. Lett.* **75** 2927

[29] Huggard P G, Shaw C J, Andrews S R, Cluff J A and Grey R 2000 *Phys. Rev. Lett.* **84** 1023

[30] Bedoya M and Camacho A S 2005 *Phys. Rev.* B **72** 155318

[31] Kinsler P, Harrison P and Kelsall R W 1999 *J. Appl. Phys.* **85** 23

[32] Autler S H and Townes C H 1955 *Phys. Rev.* **100** 703

[33] Phillips C, Su M Y, Sherwin M S, Ko J and Coldren L 1999 *Appl. Phys. Lett.* **75** 2728

[34] Johnsen K and Jauho A P 1999 *Phys. Rev. Lett.* **83** 1207

[35] Dent C J, Murdin B N and Galbraith I 2003 *Phys. Rev.* B **67** 165312

[36] Liu A and Ning C Z 2000 *J. Opt. Soc. Am.* B **17** 433

[37] Maslov A V and Citrin D S 2000 *Phys. Rev.* B **62** 16686

[38] Maslov A V and Citrin D S 2001 *Phys. Rev.* B **64** 155309

[39] Zhang J Z and Allsopp D 2009 *Phys. Rev.* B **80** 245320

[40] Kira M and Koch S 2005 *Eur. Phys. J.* D **36** 143

[41] Witthaut D and Sorensen A S 2010 *New J. Phys.* **12** 043052

[42] Shen J T and Fan S 2007 *Phys. Rev. Lett.* **98** 153003

[43] Mi X W, Cao J C and Zhang C 2004 *J. Appl. Phys.* **95** 1191

[44] Mi X W and Cao J C 2004 *Chin. Phys. Lett.* **21** 2536